

**Supplementary information for:**

**Construction of multi-dimensional flexible MnS based paper electrode with ultra-stable and high-rate capability towards efficient sodium storage**

Zehang Sun,<sup>a</sup> Yang Liu,<sup>a</sup> Dongxu Wu, Ke Tan, Linrui Hou and Changzhou Yuan\*

School of Materials Science & Engineering, University of Jinan, Jinan, 250022, P. R.

China

E-mail: mse\_yuancz@ujn.edu.cn; ayuancz@163.com

<sup>a</sup> The authors contributed equally to this work.

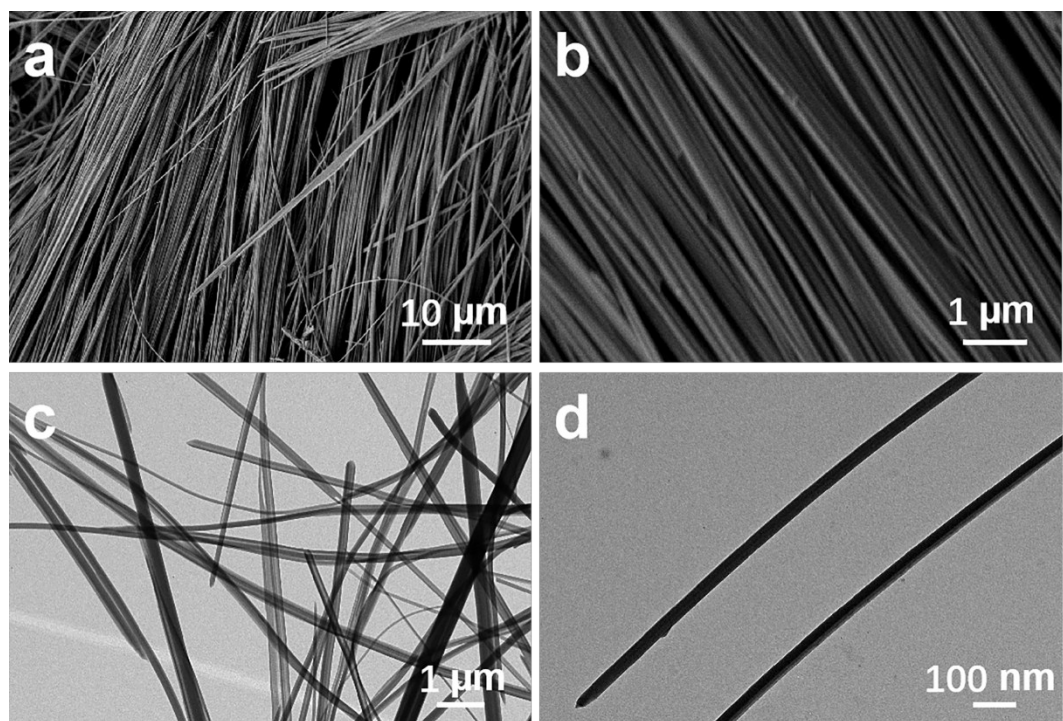


**Fig. S1** (a, b) FESEM and (c, d) TEM images of the Mn-NTA precursor

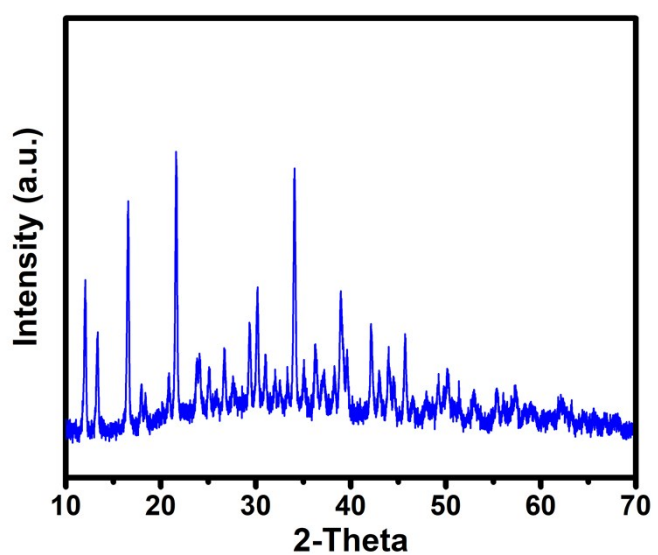


**Fig. S2** XRD pattern of the Mn-CPNWs

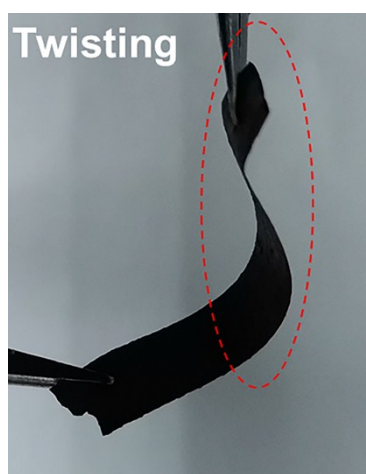


**Fig. S3** Digital images for the twisting of MnS@CNWs/rGO paper

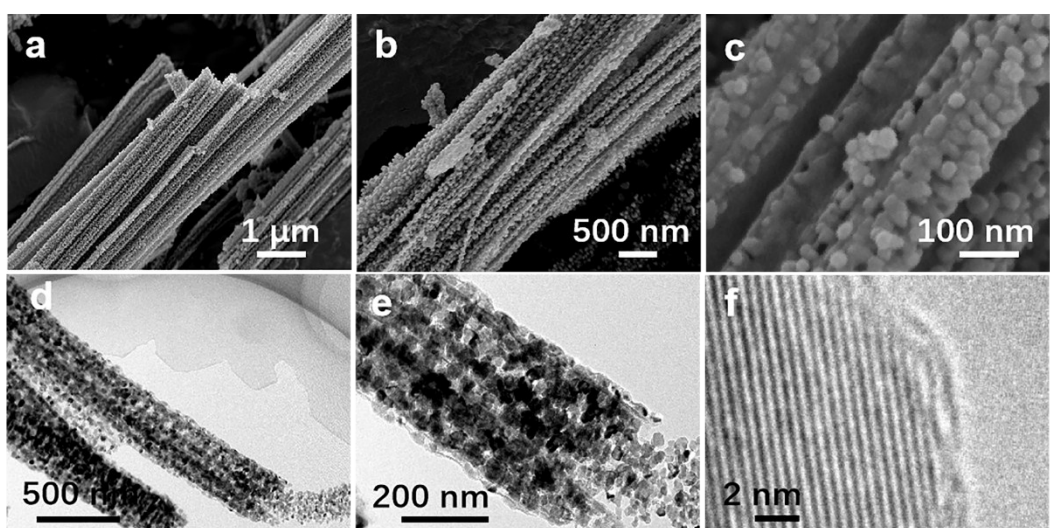


**Fig. S4** (a – c) FESEM, (d, e) TEM and (f) HRTEM images of the MnS@CNWs

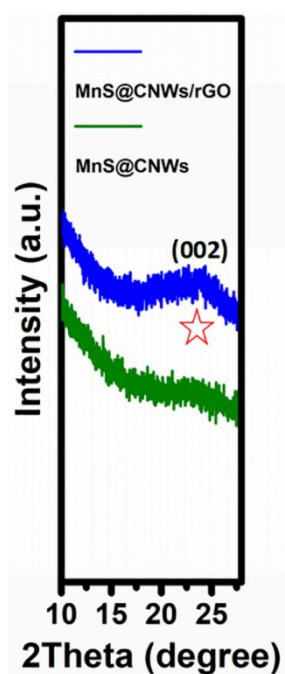


**Fig. S5** Enlarged XRD pattern ( $2\theta = 10 - 27.5$   $^{\circ}$ ) of the MnS@CNWs/rGO and MnS@CNWs

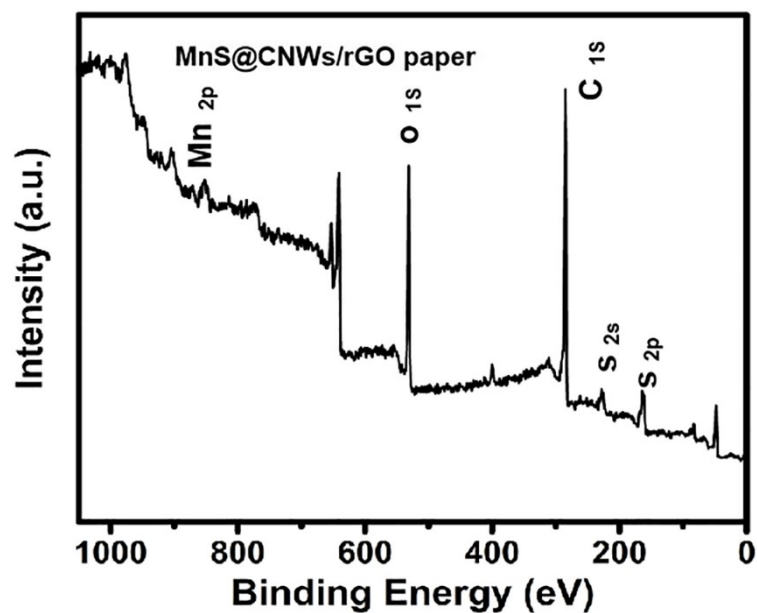


**Fig. S6** XPS survey spectrum of the MnS@CNWs/rGO

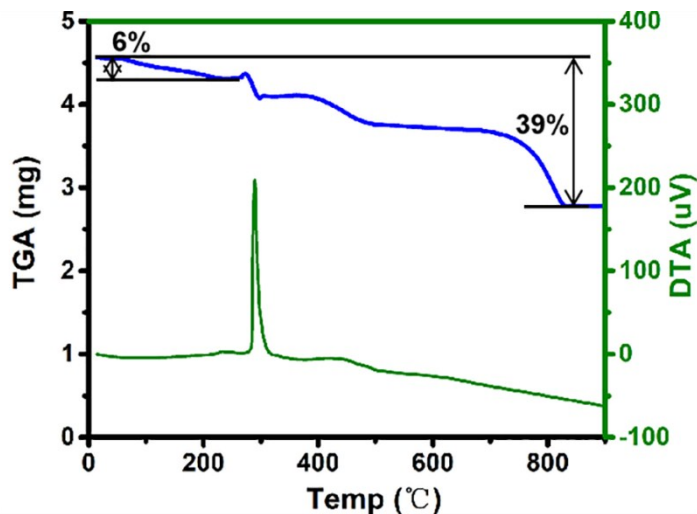


**Fig. S7** TG and DTA curves of the MnS@CNWs/rGO

In the TG curve of MnS@CNWs/rGO, a small weight loss of about 6 wt% first occurred below 100 °C because of the removal of adsorbed water on the surface of the MnS@C/rGO. Subsequently, another weight loss took place between 280 and 500 °C. It is believed that both carbon burning and MnS oxidation (transform into MnSO<sub>3</sub> and Mn<sub>3</sub>O<sub>4</sub>) occurred between 280 and 500 °C, which is consistent with previous reports.<sup>1</sup> After a plateau region, sharp weight loss was observed as the temperature increase from 700 °C to 850 °C owing to further oxidation of MnSO<sub>3</sub> and Mn<sub>3</sub>O<sub>4</sub> to Mn<sub>2</sub>O<sub>3</sub>. Based on the TGA results, the weight contents of MnS and carbon were calculated to be 71.8 wt.% and 28.2 wt.%.

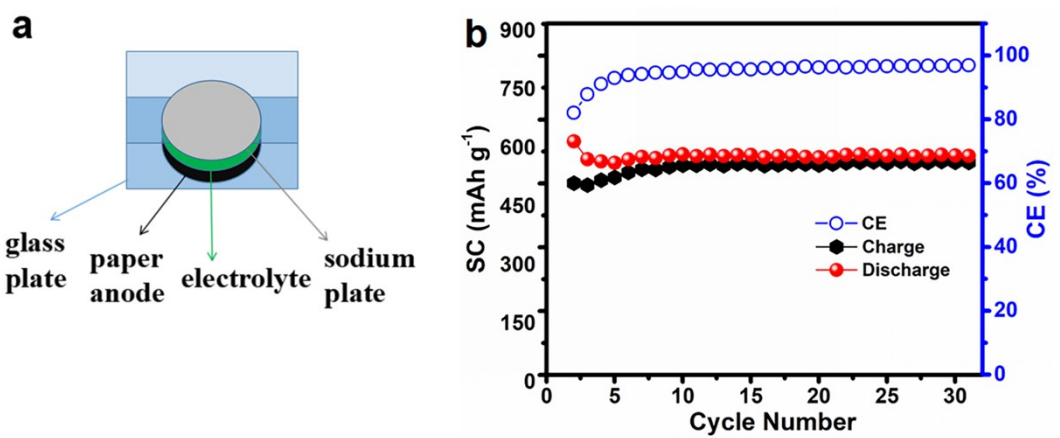


**Fig. S8** (a) Schematic illustration and (b) cycling performance ( $100 \text{ mA g}^{-1}$ ) for the pre-sodiation of  $\text{MnS@CNWs/rGO}$  paper

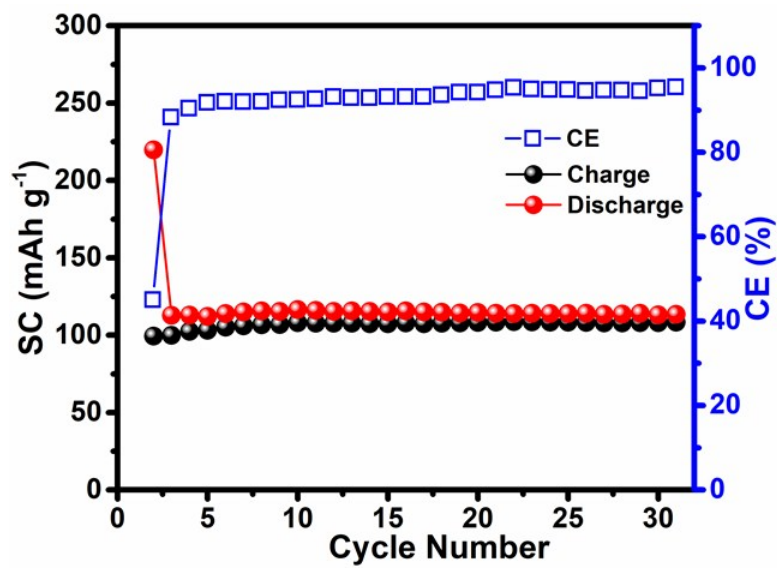


**Fig. S9** Cycling performance for the pure rGO paper at a current density of  $100 \text{ mA g}^{-1}$

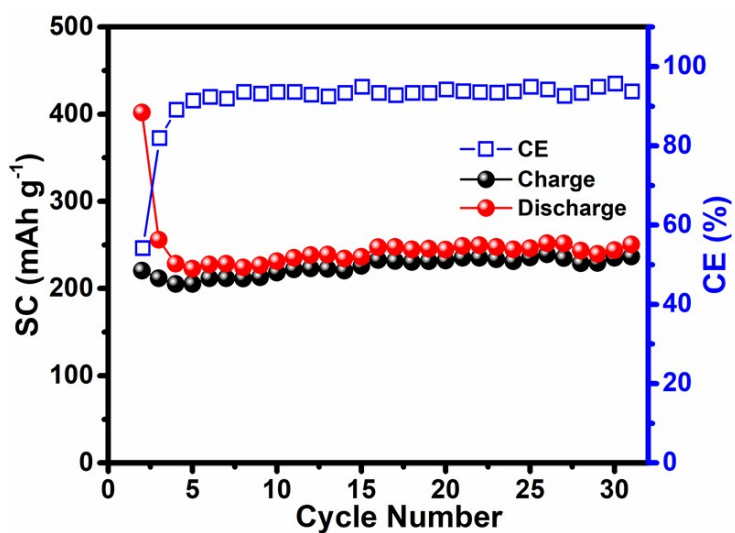


**Fig. S10** Cycling performance for the MnS@CNWs/4rGO paper at a current density of  $100 \text{ mA g}^{-1}$

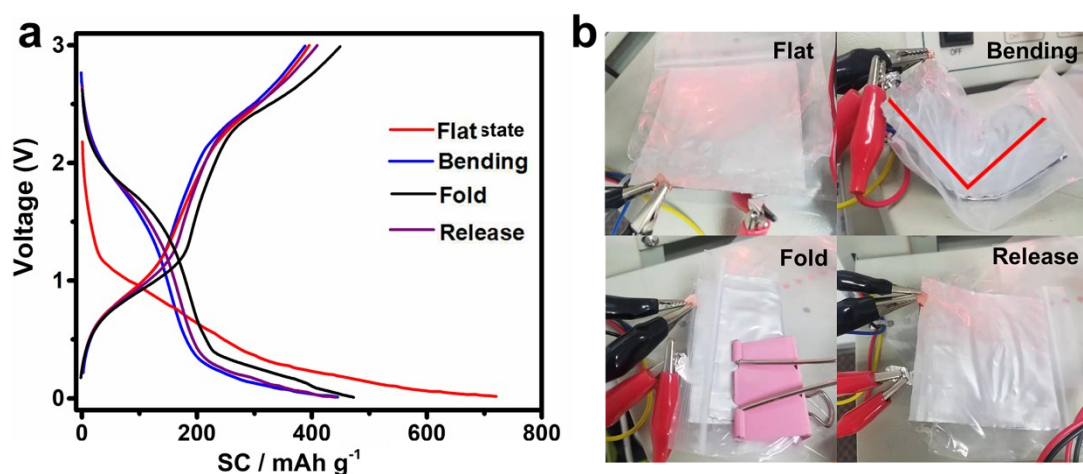


**Fig. S11** (a) Typical galvanostatic discharge-charge plots ( $100 \text{ mA g}^{-1}$ ) for (b) the soft package of half sodium ion cells in different flexible modes. The area of the MnS@CNWs/4rGO paper is  $\sim 4 \text{ cm}^2$

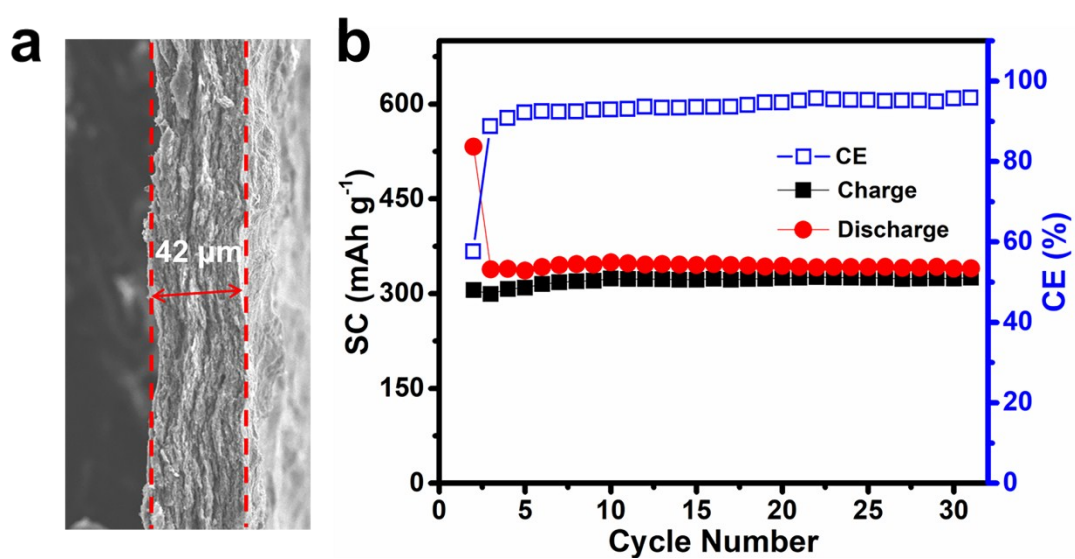


**Fig. S12** (a, b) The thickness and cycling performance ( $100 \text{ mA g}^{-1}$ ) for the MnS@CNWs/rGO paper of  $3.8 \text{ mg cm}^{-2}$

**Table S1** The comparison between this work and other sulfide self-supporting anodes for SIBs

Anode	Volumetric (areal) capacities	Mass loading (mg cm <sup>-2</sup> )	Rate capability	Cycling stability	Ref.
FeS/SPAN-HNF	—	1.5- 2.0	782.8 at 0.2 A g <sup>-1</sup>	327.5 at 5.0 A g <sup>-1</sup> after 500 cycles	2
Fe <sub>1-x</sub> S@PCNWs/rGO	424 mAh cm <sup>-3</sup> at 0.2 A g <sup>-1</sup>	0.9- 11.2	180 mAh cm <sup>-3</sup> at 5 A g <sup>-1</sup>	573 at 100 mA g <sup>-1</sup> after 100 cycles	3
3D carbon-networks/Fe <sub>7</sub> S <sub>8</sub> /graphene	2.12 mAh cm <sup>-2</sup> at 0.25 mA cm <sup>-2</sup>	—	1.12 mAh cm <sup>-2</sup> at 10.0 mA cm <sup>-2</sup>	1.064 mAh cm <sup>-2</sup> at 10.0 mA cm <sup>-2</sup> after 500 cycles	4
MWCNT and In <sub>2</sub> S <sub>3</sub> nanohybrid paper	—	1.8	280 at 1.0 A g <sup>-1</sup>	410 at 100 mA g <sup>-1</sup> after 100 cycles	5
SnS/C NFs	—	—	230 at 2.0 A g <sup>-1</sup>	349 at 200 mA g <sup>-1</sup> after 500 cycles	6
MoS <sub>2</sub> –F	—	1.0-1.2	186 at 2.0 A g <sup>-1</sup>	243 at 1000 mA g <sup>-1</sup> after 1100 cycles	7
MnS@CNF	—	1.25	87 at 1.0 A g <sup>-1</sup>	220 at 20 mA g <sup>-1</sup> after 200 cycles	8
α -MnS@N,S-NTC	—	1.5	188 at 1.0 A g <sup>-1</sup>	291 at 250 mA g <sup>-1</sup> after 200 cycles	9
MnS@CNWs/rGO	362.3 mAh cm <sup>-3</sup> at 0.1 A g <sup>-1</sup>	1.0-3.8	147 at 2.0 A g <sup>-1</sup>	≈150mA h g <sup>-1</sup> at 1000 mA g <sup>-1</sup> after 10000 cycles;	This work

Note: — : not provided; MoS<sub>2</sub>–F: MoS<sub>2</sub> and CNFs overall composite electrode

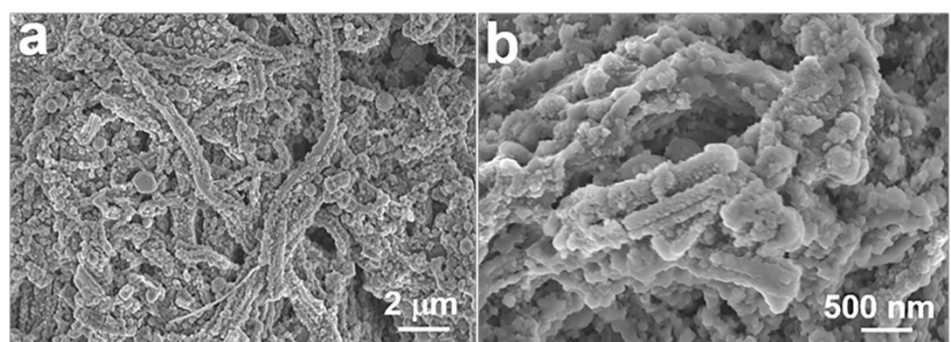


**Fig. S13** (a, b) FESEM images of the MnS@CNWs/rGO paper electrode after 50 cycle at current density of  $0.1 \text{ A g}^{-1}$

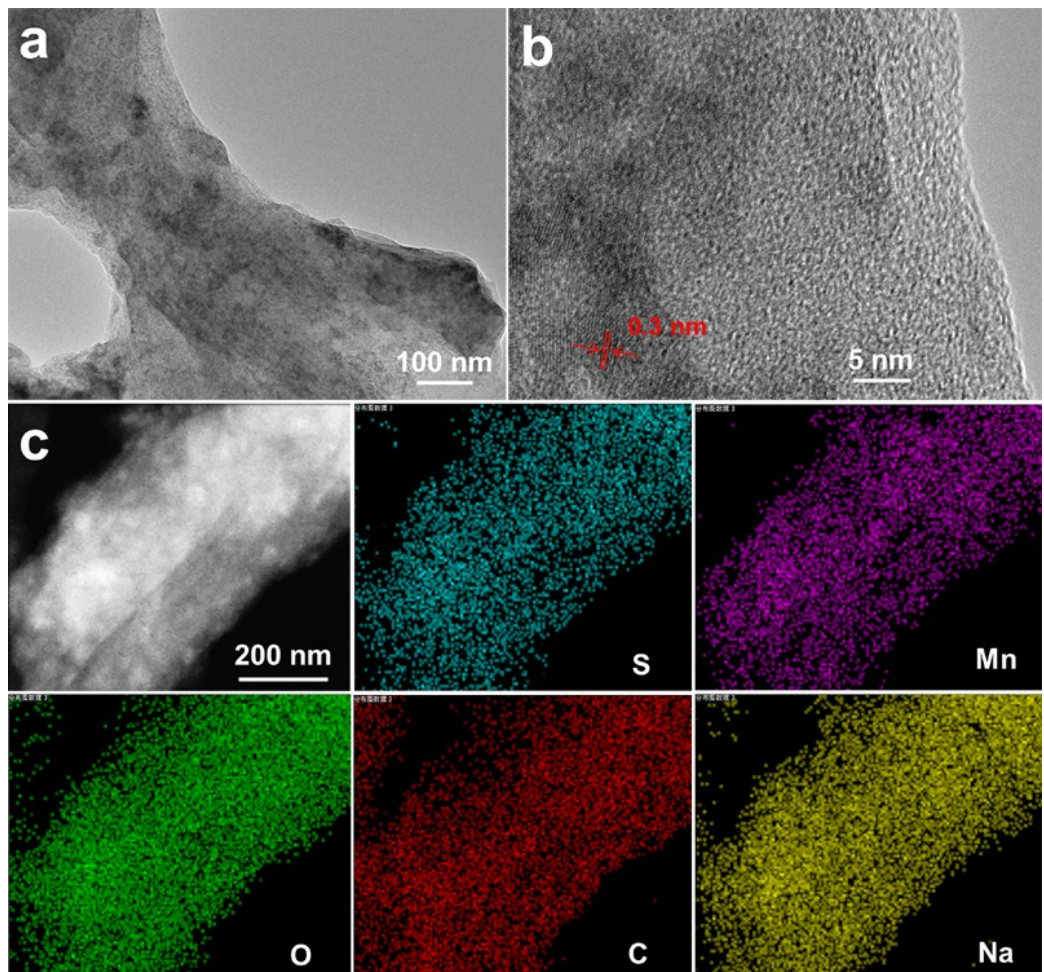


**Fig. S14** (a, b) TEM and (c) STEM images of the MnS@CNWs/rGO paper electrode after 50 cycle at current density of  $100 \text{ mA g}^{-1}$

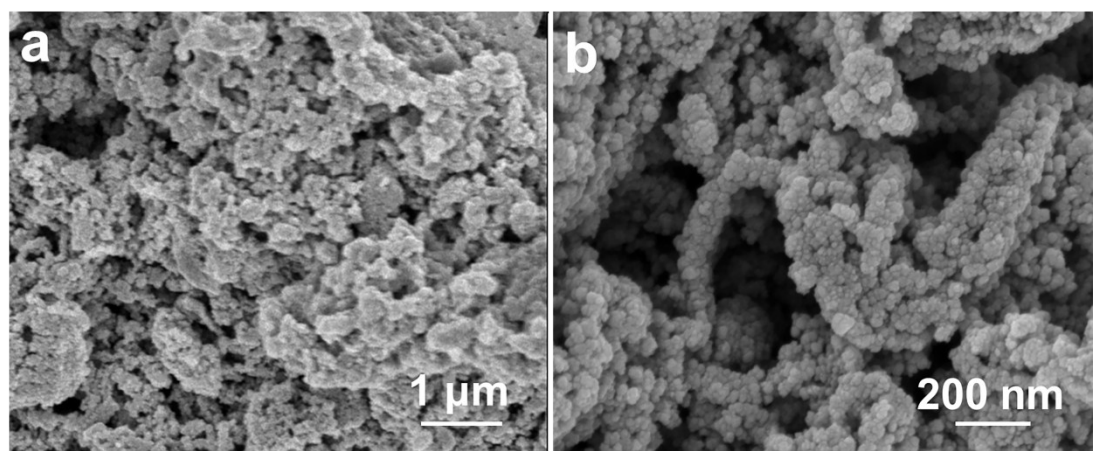


**Fig. S15** (a, b) FESEM images of the MnS@CNWs electrode after 50 cycle at current density of  $0.1 \text{ A g}^{-1}$

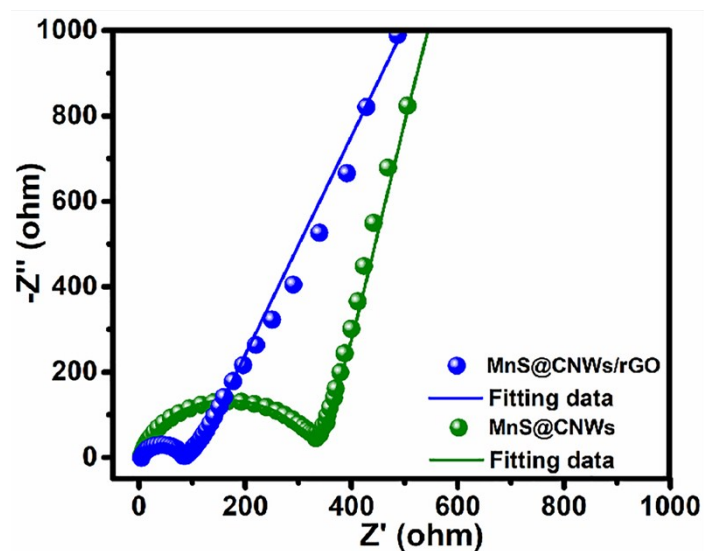


**Fig. S16** EIS spectra of the MnS@CNWs/rGO and MnS@CNWs electrodes

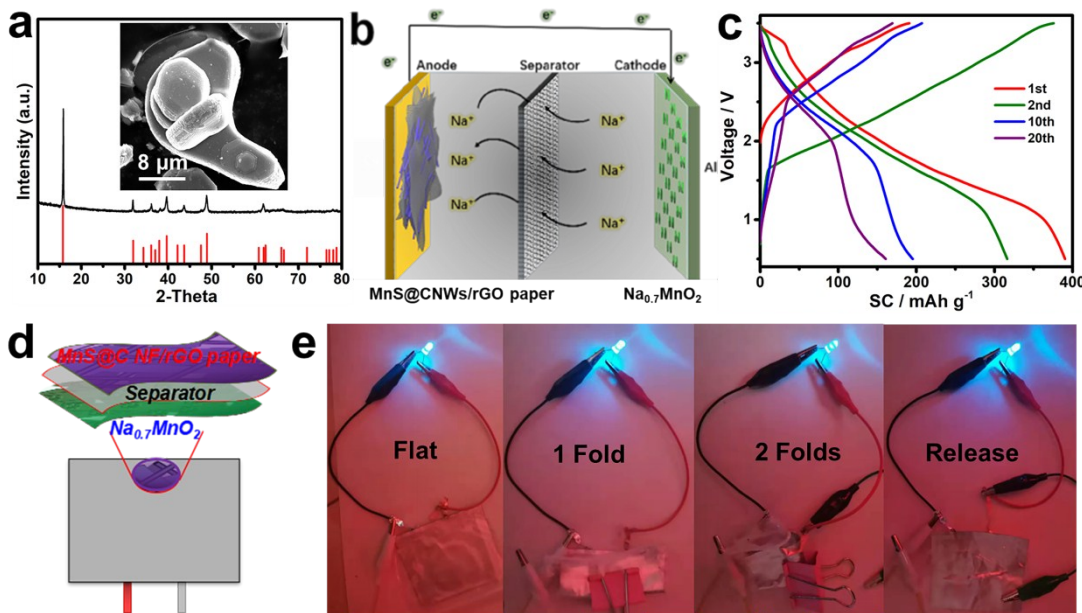


**Fig. S17** (a) XRD pattern and FESEM image (the inset) for the cathode  $\text{Na}_{0.7}\text{MnO}_2$ ; (b) Schematic illustration and (c) galvanostatic discharge-charge plots ( $100 \text{ mA g}^{-1}$ ) of the manganese-based full SIB; (d) Schematic demonstration and (e) digital pictures of the pouch-type devices in different flexible modes. The areas of the  $\text{MnS@CNWs/rGO}$  paper and the cathode  $\text{Na}_{0.7}\text{MnO}_2$  are  $\sim 4$  and  $\sim 6 \text{ cm}^2$ , respectively

## References

1. X. Xu, S. Ji, M. Gu, and J. Liu, *ACS Appl. Mater. Interfaces*, 2015, **7**, 20957-20964.
2. J. Zhang, K. Zhang, J. Yang, G.-H. Lee, J. Shin, V. W. Lau and Y. M. Kang, *Adv. Energy Mater.*, 2018, **8**, 1800283.
3. Y. Liu, Y. Fang, Z. Zhao, C. Yuan and X. W. Lou, *Adv. Energy Mater.*, 2019, **9**.1803052
4. W. Chen, X. Zhang, L. Mi, C. Liu, J. Zhang, S. Cui, X. Feng, Y. Cao and C. Shen, *Adv. Mater.*, 2019, **31**, 1806664.
5. J. Choi, Y. Myung and S. K. Kim, *Appl. Surf. Sci.*, 2019, **467-468**, 1040-1045.
6. J. Xia, L. Liu, S. Jamil, J. Xie, H. Yan, Y. Yuan, Y. Zhang, S. Nie, J. Pan, X. Wang and G. Cao. *Energy Storage Mater.*, 2019, **17**, 1-11.
7. Q. Ni, Y. Bai, S. Guo, H. Ren, G. Chen, Z. Wang, F. Wu and C. Wu, *ACS Appl. Mater. Interfaces*, 2019, **11**, 5183–5192.
8. S. Gao, G. Chen, Y. DalìAgnese, Y. Wei, Z. Gao and Y. Gao, *Chem. Eur. J.*, 2018, **24**, 13535-13539.
9. D. H. Liu, W. H. Li, Y. P. Zheng, Z. Cui, X. Yan, D. S. Liu, J. Wang, Y. Zhang, H. Y. Lu, F. Y. Bai, J. Z. Guo and X. L. Wu, *Adv. Mater.*, 2018, **30**, 1706317.